



## Effect of Laser Irradiation on Micro-Structural Properties of Zinc Ferrite

HAFIZ AKIF SHAHZAD<sup>1</sup>, YASIR JAMIL<sup>1</sup>, MUNAWAR IQBAL<sup>2,\*</sup>, MUHAMMAD MUSADIQ<sup>1</sup> and M. ASIF NAEEM<sup>1</sup>

<sup>1</sup>Department of Physics, University of Agriculture, Faisalabd-38040, Pakistan

<sup>2</sup>Department of Chemistry & Biochemistry, University of Agriculture, Faisalabd-38040, Pakistan

\*Corresponding author: E-mail: physicsuaf@yahoo.com

Received: 27 November 2012;

Accepted: 31 May 2013;

Published online: 22 March 2014;

AJC-14922

The Zn-ferrite ( $Zn_xFe_{3-x}O_4$ ) were prepared *via* co-precipitation of  $ZnCl_2$ ,  $FeCl_3 \cdot 6H_2O$  in the presence of NaOH as a precipitating agent at 90 °C. The prepared ferrites were characterized by X-ray diffraction and particle size was investigated by Sheerer's formula. The Zn-ferrites were irradiated by Nd:YAG laser and effect of laser radiation on micro-structural properties of Zn-ferrite were investigated. The particle size of unirradiated ferrites was ranged from 6 to 17 nm, while that of irradiated Zn-ferrites was found to be 5-53 nm. The minimum particle size for both radiated and irradiated sample was obtained at 0.4x of  $Zn_xFe_{3-x}O_4$ . It was found that the electrical conductivity and average lattice constants of the irradiated samples were greater in comparison to un-irradiated samples; where as the densities of the irradiated samples are less than un-irradiated samples. Results showed that the laser irradiation can be used to enhance the micro-structural properties of zinc ferrite.

**Keywords:** Zinc ferrite, Laser irradiation, XRD, Electrical conductivity, Particle size.

### INTRODUCTION

Nanomaterials have many applications in every field of life such as gas sensors<sup>1</sup>, microwave device<sup>2</sup>, photo-catalysis<sup>3</sup>, adsorption technologies<sup>4</sup>, high-frequency transformer technology<sup>5</sup>, but currently, magnetic nanoparticles offer widespread applications in biotechnology, such as DNA and RNA purification, cell separation, drug delivery, magnetic resonance imaging<sup>6</sup>, magnetic hyperthermia for cancer treatments<sup>7</sup>, thermal coagulation therapy<sup>8</sup>, biosensors<sup>9</sup>, biomolecular recognition and cell imaging<sup>10</sup>.

The soft ferrites are currently used as magnetic cores of transformers, inductors and filters to static power converters<sup>11</sup>. The magnetic properties of the magnetic materials are determined by both intrinsic magnetic and micro structural properties<sup>12,13</sup>. A number of solution-based preparation techniques are available for the preparation of fine particles (which show novel properties when compared to their properties in the bulk) with desirable size and magnetic properties<sup>14</sup>. Very fine ferrite particles can be produced by the chemical co-precipitation and sol-gel methods<sup>15</sup>. Actually, these methods demonstrated that high-density ferrite could be obtained at relatively low sintering temperature, concentration and mixing method<sup>16-18</sup>.

In present research work, we used the chemical co-precipitation method for the preparation of Zn-ferrite in the presence of NaOH as precipitating agent. The effect of radiation, concen-

tration and solution interchangeability on particle size, structural change, electrical properties and lattice constant was studied. The particle size of  $ZnFe_2O_4$  particles prepared from  $ZnCl_2$  and  $FeCl_3 \cdot 6H_2O$  was determined by Sheerer formula and density. and spacing by XRD technique.

### EXPERIMENTAL

The samples of zinc ferrite ( $Zn_xFe_{3-x}O_4$ ) powders were prepared by co-precipitation using  $ZnCl_2$  and  $FeCl_3 \cdot 6H_2O$  salts. Four samples with varying x (0.2, 0.4, 0.6 and 0.8) concentration were prepared (Table-1). The metal chlorides ( $ZnCl_2$ ,  $FeCl_3 \cdot 6H_2O$ ) and other reagent used for preparation of zinc ferrite were of analytical grade. For each sample the concentrations of NaOH and  $FeCl_3$  were kept constant. All the beakers and other apparatus were washed with deionized water and acetone.

$ZnCl_2$  and  $FeCl_3 \cdot 6H_2O$  with different quantity for different sample were dissolved in the deionized water with minimum volume and then diluted up to 50 mL. In another beaker 100 mL of solution of NaOH was prepared (2M). The beaker containing 50 mL solution of  $ZnCl_2 \cdot 4H_2O$  and  $FeCl_3 \cdot 6H_2O$  was added drop by drop into the beaker containing NaOH solution. The solution of beaker containing NaOH was placed on magnetic stirrer of moderate stirring speed (80 rpm) at room temperature. This process of adding consumed within 1 h for

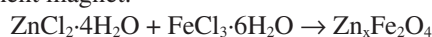
TABLE-1  
PEAK ANALYSIS OF XRD PATTERNS

Sample	Peak No.	Theta (deg)	I/I	d-value (Å)	hkl	a (Å)	FWHM [ $^{\circ}$ 2 $\theta$ ]
Sample 1 Un-irradiated	2	33.1531	53.33	2.70224	(311)	8.542	0.3149
	4	36.6909	93.33	2.4494	(222)	8.484	0.2362
	6	53.1565	57.78	1.72307	(2422)	8.441	0.3936
Sample 1 Irradiated	1	36.6052	100	2.45494	(222)	8.504	0.1574
Sample 2 Un-irradiated	1	35.5419	100	2.5259	(311)	8.377	1.2595
Sample 2 Irradiated	1	35.3101	100	2.54195	(311)	8.43	1.5744
Sample 3 Un-irradiated	1	35.5973	100	2.5221	(311)	8.364	1.2595
	2	62.6169	83.33	1.48236	(440)	8.385	2.304
Sample 3 Irradiated	1	35.3164	100	2.54151	(311)	8.429	0.6298

each sample. After this addition the final solution was 200 mL. During the addition dark brown precipitates were obtained. The pH of the solution was at 12.5.

The beaker containing the dark brown precipitates was placed into pre-heated water bath containing water. The temperature of water bath was kept at 85 °C for each sample. Digestion was performed for 90 min for different temperature. The particles were settled down at the bottom of the beaker after 90 min. The beaker was cooled to a moderate temperature after taking out from water bath. The four samples were treated with Nd:YAG Laser (Brilliant) radiation after water bath, each sample was radiated for 10 min. The solution of beaker was placed on magnetic stirrer of moderate stirring speed (50 rpm) at room temperature. For each sample the principal radiation or wavelength was 532 nm, maximum energy/pulse 200 mJ, maximum average power 2 watt, pulse duration 4ns and the Q-Switch delay was 300us.

The particles were obtained through filtration. The samples were washed with de-ionized water to obtain pH 7. This slow process was completed in 2 days. The filtered particles were dried in oven at 60 °C in 15 h. Fine particles were obtained by grinding in pestle and mortar. Before every sample, pestle and mortar was washed with acetone. Similar process was adopted to prepare the four samples. The spontaneous magnetization of the particles was checked for all the samples with the help of permanent magnet.



Finally, the powder was mixed with binder and put into dye under hydraulic press (10 Kg cm<sup>-2</sup>). The spontaneous magnetization of pellets was checked for all the samples with permanent magnet. The sample surfaces were coated by silver paste for the electrical measurements. The DC electrical conductivity was measured as a function of temperature from 20-120 °C. The prepared samples of zinc ferrites were analyzed with the help of X-ray diffraction technique<sup>19</sup>.

The particle size was measured Sherrer's formula as<sup>20</sup>:

$$2d \sin \theta = n \lambda \quad (1) \text{ Bragg's law}$$

$$B = \frac{1}{2} (2\theta_1 - 2\theta_2) = \theta_1 - \theta_2$$

The path-difference for two angles like eqn. 1, but related to entire thickness of the crystal rather than to the distance between adjacent planes can be calculated as:

$$2t \sin \theta_1 = (m + 1) \lambda$$

$$2t \sin \theta_2 = (m - 1) \lambda$$

$$t (\sin \theta_1 - \sin \theta_2) = \lambda$$

$$2t \cos (\theta_1 + \theta_2)/2 \quad \sin (\theta_1 - \theta_2)/2 = \lambda$$

$\theta_1$  and  $\theta_2$  are both nearly equal to  $\theta B$ , so that

$$\theta_1 + \theta_2 = 2 \theta B \text{ (approx.) and}$$

$$\sin (\theta_1 - \theta_2)/2 = (\theta_1 - \theta_2)/2 \text{ (approx.)}$$

$$2t (\theta_1 - \theta_2)/2 \cos \theta B = \lambda$$

$$t = \lambda / B \cos \theta B$$

$$t = 0.9 \lambda / B \cos \theta B$$

Eqn. 2 is known as the Sherrer's formula and was used to estimate the particle size of crystals by measuring the width of their diffraction curves<sup>20</sup>. X-ray densities were calculated using following formula;

$$dx = 8M/NA^{a3}$$

where "8" represents the number of molecules in a unit cell of spinel lattice, "M" is molecular mass, "a" is the lattice constant and "N" is the Avogadro's number.

**Statistical analysis:** Triplicate sample was prepared and data thus obtained was analyzed statistically to calculate the level of significance of various parameters using analysis of variance technique by Minitab Software Package Version 14.0 (Minitab, Inc., State College, PA, USA) at 95 % confidence interval of mean and data were reported as Mean  $\pm$  SD.

## RESULTS AND DISCUSSION

The reaction condition, preparation and concentration can influence the particle size, shape, electrical properties and crystallization of the precipitated ferrites. All sample of Zn-ferrite prepared by co-precipitation was found to be highly magnetic. Similar results have also been reported by Hsu *et al.*<sup>21</sup> for nano ferrite prepared by co-precipitation method. Figs. 1 and 2 showing the X-ray diffraction patterns of the precipitated Zn<sub>x</sub>Fe<sub>2</sub>O<sub>4</sub>, which revealed that the laser incidence increase the size of nano ferrites which were prepared at different ratios of Zn and Fe concentration and their properties are shown in Table-1. The XRD pattern recorded for the un-irradiated sample 1 in pellet form after a digestion temperature of 90 °C for 6 h (x = 0.2).

The characteristic peaks at  $2\theta$  values for unirradiated sample were found 34.8322, 36.6909 and 53.1565 having Miller indices (311), (222) and (422), respectively, which were in close agreement with characteristic peaks of ferrites when compared with ICSD card (with codes 00-001-1121, 00-002-1045 and 00-003-0664), which clearly indicates the formation of spinal cubic ferrite of CoZnFe<sub>2</sub>O<sub>4</sub>. Similar, results have also been reported by Mathur *et al.*<sup>22</sup>. The XRD patterns of radiated sample showed the characteristic peaks at  $2\theta$  value 36.6052° having Miller indices (311). The disappearance of peaks at 36.7° and 53° indicated the formation of distorted cubic structure. For sample number 2 (un-irradiated), the XRD pattern

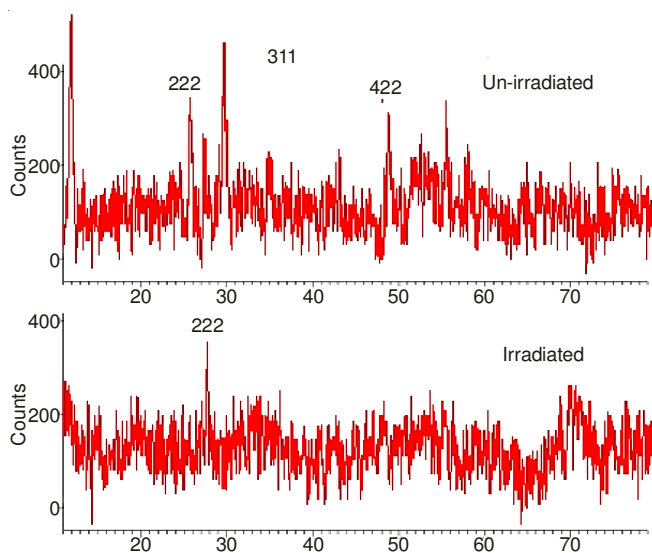


Fig.1. XRD pattern of Zn-ferrite

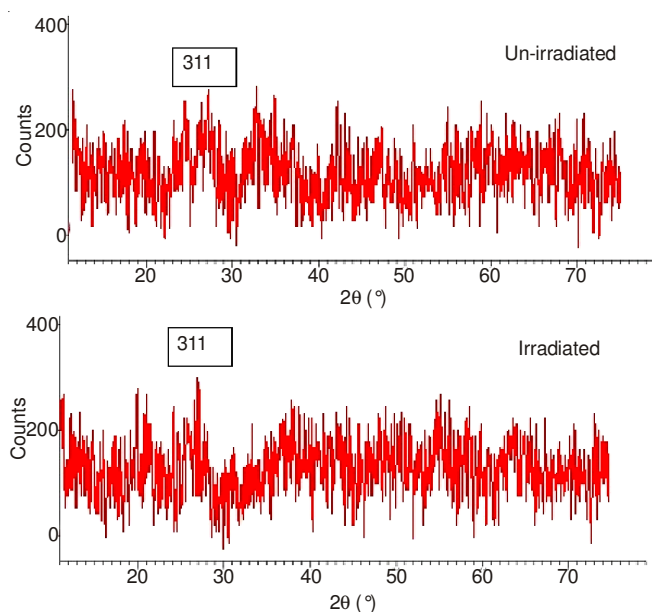


Fig.2. XRD pattern of Zn-ferrite, when X = 0.4

of synthesized sample showed the characteristic peak at  $2\theta$  value  $35.54^\circ$  having Miller indices (311). The laser irradiation generates localized hopping electrons which help the production of  $\text{Fe}^{2+}$ , at the octahedral configuration (sites) as follows:  $\text{Fe}^{3+} + \text{Laser} \rightarrow \text{Fe}^{2+} + e^-$ . This causes more contribution towards conductivity by generation of localized hopping electrons and holes. The ionic size of  $\text{Fe}^{2+}$  is larger than that of  $\text{Fe}^{3+}$ , leading to distortion of the spinel cubic structure.

Moreover, lattice vacancies generated after irradiation causes distortion and deviation from the spinel cubic structure<sup>23</sup>. The sample number 3 was found different and it showed very small change in XRD pattern at  $2\theta$  values 35.5973, 62.6169 and Miller Indices (311), (440) for un-irradiated and  $2\theta$  values 35.3164, 62.7793 for radiated sample with Miller indices.

The electrical conductivity measured in terms of resistivity decreased with the increase in temperature as shown in the Fig. 3. Further the irradiated sample found good conductor as

compared to un-irradiated<sup>23,24</sup>. The trend of change in particle diameter with for different concentrations of  $x$  (0.2, 0.4 0.6 and 0.8) is shown in Fig. 4. The increase in particle size after laser irradiation was found higher for sample 1 with lower ratio of  $x$  (0.2). The X-ray density was found to decrease by increasing Zn concentration in both the cases (metal ion solution in burette and flask). The porosity is the ratio of measured density and X-ray density  $P = 1 - (\rho_m/\rho_x)$ . The average porosity was found to be 0.21-0.25, which is in close agreement<sup>25</sup>.

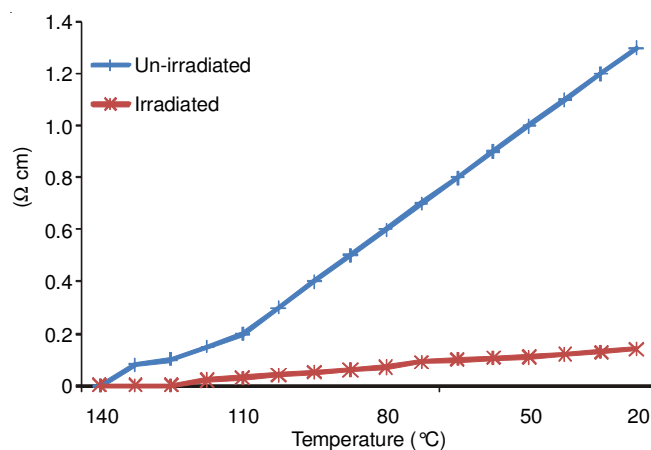
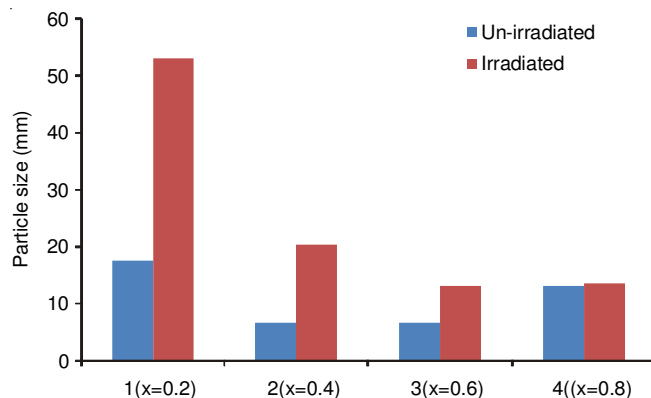
Fig. 3. Electrical conductance of Zn-ferrite ( $\text{Zn}_x\text{Fe}_{3-x}\text{O}_4$ ),  $x = 0.2$ 

Fig. 4. Variation in particle size on laser radiation of different samples

The co-precipitation technique was successfully employed for the preparation of Zn-ferrite ( $\text{Zn}_x\text{Fe}_{3-x}\text{O}_4$ ). The laser irradiation caused increase in particle size, which was found smaller for samples having higher  $\text{Zn}^{2+}$  concentrations and transformation of spinel structure into distorted cubic structure. Furthermore, the electrical conductivity increased with laser irradiation which might be found useful for engineering purposes.

## REFERENCES

1. N. Rezlescu, C. Doroftei, E. Rezlescu and P.D. Popa, *Sens. Actuators B*, **133**, 420 (2008).
2. Z. Yao, P. Li and C. Jiang, *J. Magn. Magn. Mater.*, **321**, 203 (2009).
3. H. Yang, J. Yan, Z. Lu, X. Cheng and Y. Tang, *J. Alloys Comp.*, **476**, 715 (2009).
4. A. Kraus, K. Jainae, F. Unob and N. Sukpirom, *J. Colloid Interf. Sci.*, **338**, 359 (2009).
5. K. Praveena, K. Sadhana, S. Bharadwaj and S.R. Murthy, *J. Magn. Magn. Mater.*, **321**, 2433 (2009).

6. T. Tanaka, R. Shimazu, H. Nagai, M. Tada, T. Nakagawa, A. Sandhu, H. Handa and M. Abe, *J. Magn. Magn. Mater.*, **321**, 1417 (2009).
7. W.C. Kim, S.L. Park, S.J. Kim, S.W. Lee and C.S. Kim, *J. Appl. Phys.*, **87**, 6241 (2000).
8. H. Hirazawa, S. Kusamoto, H. Aono, T. Naohara, K. Mori, Y. Hattori, T. Maehara and Y. Watanabe, *J. Alloys Comp.*, **461**, 467 (2008).
9. M. Pita, J.M. Abad, C. Vaz-Dominguez, C. Briones, E. Mateo-Martí, J.A. Martín-Gago, M. del Puerto Morales and V.M. Fernández, *J. Colloid Interf. Sci.*, **321**, 484 (2008).
10. M. Hatakeyama, Y. Mochizuki, Y. Kita, H. Kishi, K. Nishio, S. Sakamoto, M. Abe and H. Handa, *J. Magn. Magn. Mater.*, **321**, 1364 (2009).
11. E. Cardelli and E. Della Torre, *Physica B*, **306**, 240 (2001).
12. T. Schrefl, W. Suess, H. Forster, V. Tsiantos and J. Filder, Finite element micromagnetics, In: Lecture Notes in Computational Science and Engineering 28, Springer, pp. 165-181 (2003).
13. M.-W. Moon, S.H. Lee, J.-Y. Sun, K.H. Oh, A. Vaziri and J.W. Hutchinson, *Scripta Mater.*, **57**, 747 (2007).
14. R. Arulmurugan, G. Vaidyanathan, S. Sendhilnathan and B. Jeyadevan, *Physica B*, **363**, 225 (2005).
15. C.S. Kim, W.C. Kim, S.Y. An and S.W. Lee, *J. Magn. Magn. Mater.*, **215**, 213 (2000).
16. X.H. Wang, 103<sup>rd</sup> Annual Meeting of American Ceramics Society; Indianapolis, USA, p. 22 (2001).
17. C.W. Kim and J.G. Koh, *J. Magn. Magn. Mater.*, **257**, 355 (2003).
18. S.R. Murthy and A. Mater, *J. Mater. Sci. Lett.*, **21**, 657 (2002).
19. L.A. Wahab and H.H. Amer, *Egypt. J. Solids*, **28**, 255 (2005).
20. B.D. Cullity, Elements of X-ray Diffraction, Addison-Wesley, Reading, MA (1978).
21. W.-C. Hsu, S.C. Chen, P.C. Kuo, C.T. Lie and W.S. Tsai, *Mater. Sci. Eng. B-Solid*, **111**, 142 (2004).
22. P. Mathur, A. Thakur and M. Singh, *Z. Phys. Chem.*, **221**, 887 (2007).
23. A. Tawfik, I.M. Hamada and O.M. Hemeda, *J. Magn. Magn. Mater.*, **250**, 77 (2002).
24. M.A. Mousa, A.M. Summan, M.A. Ahmed and A.M. Badawy, *J. Mater. Sci.*, **24**, 2478 (1989).
25. I.H. Gul, A.Z. Abbasi, F. Amin, M. Anis-ur-Rehman and A. Maqsood, *J. Magn. Magn. Mater.*, **311**, 494 (2007).